Journal of Nuclear Materials 557 (2021) 153260

Contents lists available at ScienceDirect

Journal of Nuclear Materials

journal homepage: www.elsevier.com/locate/jnucmat

Chemical transformations of UF_4 under controlled temperature and relative humidity

Kevin J. Pastoor[a], Michael J. Dzara[a], Svitlana Pylypenko[a], Jenifer C. Shafer[a,b,*], Mark P. Jensen[a,b,*]

[a] Department of Chemistry, Colorado School of Mines, Golden, Colorado 80401, United States
[b] Nuclear Science and Engineering Program, Colorado School of Mines, Golden, Colorado 80401, United States

ARTICLE INFO

Article history:
Received 22 June 2021
Revised 10 August 2021
Accepted 17 August 2021
Available online 19 August 2021

Keywords:
Uranium tetrafluoride
Nuclear fuel cycle
Nuclear forensics
Powder X-ray diffraction
X-ray photoelectron spectroscopy

ABSTRACT

Uranium tetrafluoride (UF_4) is a critical compound in the nuclear fuel cycle, particularly as an intermediate in uranium hexafluoride (UF_6) and uranium metal production, and as a fuel for fluoride-based molten salt reactors. Changes to UF_4 in humid air were investigated by aging anhydrous UF_4 under various temperature and relative humidity (RH) conditions for up to 9 months. Powder X-ray diffraction (pXRD) and thermogravimetric analysis revealed UF_4 remained largely unchanged during the aging study for most of the conditions investigated (293 and 308 K, and ≤75% RH), consistent with the conventional consideration that UF_4 is stable under ambient conditions. However, aging under high RH conditions (>90%) resulted in chemical speciation changes and formation of UF_4 and UF_4 hydrate mixtures. Specifically, $UF_4{\cdot}2.5H_2O$ was formed within 30 days for UF_4 aged at 293 K and 95% RH. Uranium tetrafluoride hydrates with less than 2.5 waters of hydration were formed within 180 days for UF_4 aged at 308 K and 91% RH. These findings represent the first report of UF_4 hydrates forming from the reaction of UF_4 with atmospheric water vapor at ambient temperatures. Investigation of the surface composition of unaged and aged UF_4 samples with X-ray photoelectron spectroscopy revealed degradation of the UF_4 surface, consistent with the degradation observed for the bulk UF_4 from the pXRD measurements. From a nuclear forensics perspective, these short timeline aging studies suggest that the presence of UF_4 hydrate in UF_4 materials may indicate it was stored under high humidity conditions.

1. Introduction

Increasing understanding of the physical and chemical characteristics of nuclear fuel cycle materials is an important area of research for the nuclear industry, the field of nuclear forensics, and nuclear nonproliferation efforts [1–3]. Recent work has investigated elemental and chemical impurities in various uranium oxides and uranium ore concentrates (UOCs) to determine if they can be leveraged to determine the origin and process history of a uranium material [4–14]. Another recent focus has been on the morphology of various uranium oxides and UOCs, with an aim to discern their process history [15–20]. A remaining gap in these areas of research has been understanding chemical and physical changes that may occur in nuclear materials during periods of storage and transportation.

To address this gap, an emerging area of research is the characterization of environmentally driven changes in fuel cycle relevant uranium compounds, for example changes in the parent material arising from exposure to atmospheric water vapor, precipitation, or UV light. To-date, particular focus has been given to uranium oxides and UOCs, and efforts have identified changes in both chemical speciation and morphology for uranium oxides exposed to various environmental conditions [21–26]. In the nuclear fuel cycle, such transformations can affect the processability of uranium-bearing materials [27]. For nuclear forensics purposes, on the other hand, any chemical or physical changes could serve as indicators of exposure to certain environmental conditions, potentially as a chronometer for assessing the time elapsed since a uranium compound was produced, and help ascertain aspects of a material's provenance. In particular, water exposure has been observed to play a critical, recurrent role in the environmentally driven changes to uranium compounds [21,23–29].

Uranium tetrafluoride (UF_4) is a critical compound in the nuclear fuel cycle, particularly as a precursor in the production of

* Corresponding authors.
E-mail addresses: jshafer@mines.edu (J.C. Shafer), mjensen@mines.edu (M.P. Jensen).

https://doi.org/10.1016/j.jnucmat.2021.153260
0022-3115/

uranium hexafluoride (UF_6), which is required for uranium enrichment. However, UF_4 has been significantly less studied and characterized than either uranium oxides or UF_6. Historically, UF_4 has been considered stable under ambient conditions, but two recent studies using micro-Raman spectroscopy investigated UF_4 particles exposed to various environmental conditions and identified possible degradation pathways [30]. Wellons et al. observed differing pathways depending on storage conditions and duration where short-term storage (approximately 2 weeks) under moderate relative humidity (RH, 50%) converted UF_4 to UO_2F_2 followed by formation of a schoepite compound (either metaschoepite $[(UO_2)_4O(OH)_6](H_2O)_5$ or schoepite $[(UO_2)_4O(OH)_6](H_2O)_6$), and finally uranium oxide (U_xO_y), but UO_2F_2 was not observed at higher RH (85%) conditions [29]. A longer duration (approximately 7 weeks) study resulted in the eventual formation of a uranyl peroxide ($UO_2(O_2)\cdot 2H_2O$). Pointurier et al. completed a 3-month aging study and observed the formation of a schoepite compound; adding UV exposure resulted in the formation of a uranyl peroxide under humid conditions (>74% RH) [28]. Overall, these studies indicate micron sized UF_4 particles are likely to undergo environmentally driven changes in chemical speciation and these possible degradation pathways involve significant changes in chemical speciation including oxidation of uranium, fluorine loss, and uranium-oxo bond formation.

Given the studies by Wellons et al. and Pointurier et al. of micron sized UF_4 particles, a remaining question was whether bulk quantities of UF_4 exposed to various environmental conditions would exhibit similar changes in chemical speciation. The goal of this work is to determine if bulk scale UF_4 would undergo environmentally driven degradation and if so, identify the degradation pathway. Samples of UF_4 were aged at controlled temperature and RH conditions for up to 9 months. Powder X-ray diffraction (pXRD) and thermogravimetric analysis (TGA) were used to characterize any changes to the bulk material and X-ray photoelectron spectroscopy (XPS) was used to investigate any changes to the surface of the UF_4. Based on previous studies of uranium oxides and UOCs, it is expected that high relative humidity (RH) conditions are necessary for any changes in speciation to occur.

2. Experimental

2.1. Materials

Caution: Solid uranium compounds are a dispersible radioactive material and should only be handled by those who have received applicable radiation safety training. The UF_4 used for this work was purchased from International Bio-Analytical Industries, Inc. (IBI Labs). The as received powder was stored in a dry, inert (Ar) atmosphere until used. Potassium nitrate (>99.0%), lithium chloride (>99.0%), zinc oxide (>99.9%), and trace metal grade hydrofluoric acid were purchased from Sigma-Aldrich. Sodium chloride (>99.0%), magnesium chloride (>99.0%), and hydrogen peroxide (30%) were purchased from Fisher Chemical. Uranyl nitrate hexahydrate and trace metal grade Ultrex II nitric acid were purchased from J.T. Baker. Ultrapure water (18 MΩ) was produced by a Millipore water purification system.

Uranyl fluoride (UO_2F_2) was synthesized using a modified procedure based on previous work by Chakravorti et al. [31]. Uranyl nitrate hexahydrate [$UO_2(NO_3)_2\cdot 6H_2O$, 9.3 g] was dissolved in 50 mL of 18 MΩ water and 0.3 mL of 70 wt % HNO_3. The solution was heated to 343 K and 5 mL of 30% H_2O_2 was added dropwise while stirring. A bright yellow precipitate formed, and the reaction was stirred for an additional 30 minutes at 343 K. The precipitate was isolated using vacuum filtration and subsequently washed repeatedly with 18 MΩ water. After drying, the purity of the uranyl peroxide [$(UO_2)O_2\cdot 2H_2O$] precipitate was confirmed via pXRD. The

Table 1
UF_4 aging temperature and RH conditions; RH values were determined by Greenspan [32].

Saturated Salt Solution	Relative Humidity at 293 K (%)	Relative Humidity at 308 K (%)
KNO_3	95	91
NaCl	75	75
$MgCl_2$	33	32
LiCl	11	11

($UO_2)O_2\cdot 2H_2O$ (6.4 g) was transferred to a perfluoroalkoxy alkanes (PFA) Erlenmeyer flask and dissolved in 4.5 mL of trace metals concentrated HF and 5.5 mL of 18 MΩ water. The flask was agitated by hand until the ($UO_2)O_2\cdot 2H_2O$ was fully dissolved. The reaction was evaporated to dryness on a hotplate. The resulting solid was ground using a mortar and pestle, then dried under vacuum at 373 K for 48 hours. The product (UO_2F_2) was verified using pXRD and Raman spectroscopy.

2.2. UF_4 aged under controlled temperature and relative humidity (RH) conditions

Samples of UF_4 were aged under the atmospheric conditions shown in Table 1. For each storage condition, UF_4 samples were aged for 30, 90, 180, or 270 days. The aging container system was comprised of 60 mL PFA jars containing approximately 10 mL of an aqueous saturated salt solution. Various saturated salt solutions were used to control the RH inside the container and are outlined in Table 1. Three mL PFA vials containing approximately 0.5 g of the UF_4 starting material were placed, uncapped, inside the PFA jars, exposing the UF_4 to the controlled atmosphere. The jars were sealed using PFA screw caps and secured with parafilm. The room temperature samples were stored on a laboratory surface; laboratory climate control maintains an ambient temperature of 293 ± 1 K. The elevated temperature samples were completely submerged in a bead bath, maintained at 308 ± 1 K. Temperatures were monitored using a Elitech RC-5+ temperature data logger. All samples were covered to protect them from ambient light. At the desired aging time, the vial of aged UF_4 was removed from the aging container and the material was promptly analyzed.

2.3. Powder X-ray diffraction (pXRD) and thermogravimetric analysis (TGA)

The UF_4 starting material and aged UF_4 samples were analyzed using pXRD and TGA to identify changes in chemical speciation. Powder-XRD patterns were collected on a Bruker D2 Phaser diffractometer equipped with a Lynxeye silicon strip detector and using mono-chromatic Cu Kα X-rays. An air sensitive sample holder equipped with a knife edge beam stop was used to prevent contaminating the diffractometer with uranium. Each pXRD pattern was collected over 10-80° 2θ using a step size of 0.01° and a step rate of 0.5 sec/step. Powder pattern analyses were performed using PanAlytical HighScore Plus and the PDF-2 2016 database from the International Centre for Diffraction Data [33,34].

Thermogravimetric analysis was performed using a NETZSCH STA 449 F3 Jupiter instrument. Samples were heated at 10 K per minute under a flow of argon to a maximum temperature of 623 K. The free water content for all samples was determined by the % mass loss at 373 K and waters of hydration were determined by the % mass loss over 373 – 623 K.

2.4. X-ray photoelectron spectroscopy (XPS) Analysis

X-ray photoelectron spectroscopy measurements were performed on a custom Scienta-Omicron HiPP-3 system operating in

transmission mode using an Al Kα X-ray (1486.6 eV) excitation source and a R4000 hemispherical analyzer. The system was calibrated to the Au 4f region of a sputter cleaned Au foil. The X-ray source was operated with a 900 µm spot size at 300 W. Survey spectra were recorded at a pass energy of 200 eV with a slit size of 4.0 mm x 30 mm and a step size of 1.0 eV for an estimated energy resolution of 2.0 eV; core level measurements were performed at a 200 eV pass energy with a 0.8 mm x 30 mm slit size and a 0.1 eV step size resulting in an estimated energy resolution of 0.59 eV. The analysis chamber pressure was maintained below 5.0×10^{-8} mbar, while the analyzer pressure was maintained below 1×10^{-9} mbar. Charge compensation was achieved using a low energy electron source operating at 50 µA and an energy of 10.0 eV. All UF_4, aged UF_4, and UO_2F_2 samples were mounted on insulating double-sided tape in order to electrically insulate the sample to aid in charge neutralization. Data analysis and quantification were performed using CasaXPS software. A Shirley background was applied to all high-resolution, core level spectra. The relative quantification values (elemental ratios) are ratios of the area under the curve for the element's respective core level. The elemental ratios are not expected to match the chemical formula for a given compound due to varying sensitivity of the instrument to different elements. Standard deviation was estimated from triplicate measurements, each performed on unique areas of the sample to account for possible heterogeneity of the material.

3. Results and discussion

3.1. Chemical speciation of UF_4 aged under controlled temperature and RH conditions

To determine whether bulk anhydrous UF_4 undergoes environmentally driven changes, aging containers were assembled to investigate various temperature (293 and 308 K) and relative humidity conditions (11 – 95% RH) that could be encountered in the terrestrial environment. Samples of commercially available anhydrous UF_4 from IBI Labs were exposed to the various conditions for up to 9 months. Powder-XRD phase identification analysis of the commercially acquired anhydrous UF_4 verified the starting material was UF_4 and contained no other crystalline phases (Figs. 1 and S1). After aging 30 days, pXRD analysis indicated there had been no changes in chemical speciation for all aging conditions, except for the sample aged at 293 K and 95% RH (Figs. 1, 2, and S2 – S7). For that sample, a new diffraction peak was present at approximately $2\theta = 10.6°$, however the diffraction peak was of very low intensity and the identity of the new crystalline phase could not be determined. Following 90 days aging, pXRD analysis again showed no changes had occurred for all conditions except the sample stored at 293 K and 95% RH. The previously observed diffraction peak at $2\theta = 10.6°$ increased in intensity and several new diffraction peaks were present. The new crystalline phase in the sample was identified as a uranium tetrafluoride hydrate ($UF_4{\cdot}2.5H_2O$), indicating that the aged sample was a mixture of UF_4 and $UF_4{\cdot}2.5H_2O$. Similarly, after 180 days of storage, pXRD analysis indicated no changes had occurred for most of the aging conditions. For the sample stored at 293 K and 95% RH, the diffraction peaks corresponding to $UF_4{\cdot}2.5H_2O$ had significantly increased in intensity and the diffraction peaks corresponding to UF_4 had decreased in intensity, indicating the fraction of $UF_4{\cdot}2.5H_2O$ in the aged sample had increased. For the UF_4 stored at 308 K and 91% RH, new diffraction peaks were present at approximately $2\theta = 31.1°$ and 31.6°; however, the limited number of new peaks precluded the identification of the new crystalline phase(s). Powder-XRD analysis of the samples aged for 270 days, the maximum aging time in this study, again indicated no changes in chemical speciation for most aging conditions. The peak intensities corresponding to $UF_4{\cdot}2.5H_2O$ further increased in intensity for the sample stored at 293 K and 95% RH. More significant changes were observed for the sample stored at 308 K and 91% RH, with diffraction peaks present at approximately $2\theta = 12.7°$, 31.1°, 31.6°, 44.9°, and 45.1°. Phase identification indicated several possible compounds that could correspond to the new diffraction peaks in the 308 K and 91% RH sample including $UF_4{\cdot}1.2H_2O$, $UF_4{\cdot}1.3H_2O$, $UF_4{\cdot}1.5H_2O$ and $U_3F_{12}{\cdot}H_2O$. However, due to similarities between the diffraction patterns for the possible UF_4 hydrates, the new phase(s) present in the aged sample could not be determined with certainty.

3.2. Quantitative phase analysis (QPA) and TGA analysis of UF_4 and aged UF_4 samples

Changes in the pXRD patterns for this study were quantified via Rietveld refinement using the internal standard method. Uncertainties are estimated standard deviations from Rietveld refinement. For QPA using an internal standard, the samples were spiked with approximately 20 wt % of ZnO. Using the calculated and known wt % of the internal standard, the calculated wt % of the other crystalline phases is corrected according to Eq 1, where $W_{i,c}$ is the corrected mass fraction of phase i, W_i is the calculated mass fraction of phase i, W_s is the calculated mass fraction of the internal standard, $W_{s,w}$ is the actual mass fraction of the internal standard [35–37]. Additionally, the internal standard method is particularly useful because it enables quantification of the amorphous phase which is not directly detected via pXRD. If the amorphous phase is not accounted for, QPA will overestimate the crystalline phases in the sample. The wt % of the amorphous phase is determined according to Eq 2, where W_a is the mass fraction of the amorphous phase.

$$W_{i,c} = W_i \frac{W_{s,w}}{W_s}\left(\frac{1}{1 - W_{s,w}}\right) \quad (1)$$

$$W_a = 1 - \sum_i W_{i,c} \quad (2)$$

The QPA results for the various aging conditions are shown in Figs. 3, 4, and S8 – S46. The results confirmed the qualitative pXRD observation that for UF_4 aged at 293 K and 95% RH, the fraction of $UF_4{\cdot}2.5H_2O$ in the sample increased with additional aging time (Fig. 3). In particular, the fraction of $UF_4{\cdot}2.5H_2O$ increased significantly, from approximately 3 to 33%, during the 90 days that elapsed between the 90- and 180-day checks. The fraction of $UF_4{\cdot}2.5H_2O$ continued to increase during the 90 days that elapsed between 180 and 270 days, but only increased from approximately 33 to 40%, indicating the system is likely approaching the maximum fraction of $UF_4{\cdot}2.5H_2O$ that will be formed at 293 K and 95% RH. Additional aging time would be required to determine the maximum concentration of $UF_4{\cdot}2.5H_2O$ for these conditions.

As discussed in the previous section, the precise UF_4 hydrates in the UF_4 aged for 270 days at 308 K and 91% RH could not be determined with certainty. In order to provide an estimate of the UF_4 hydrates present, QPA was performed assuming $UF_4{\cdot}1.2H_2O$ and $UF_4{\cdot}1.5H_2O$ were the only new phases present. These hydrates were chosen because they best match the new peaks at $2\theta = 31.1°$, 31.6°, 44.9°, and 45.1°. For this approach, the QPA results for the UF_4 aged for 270 days at 308 K and 91% RH estimated the sample contained 16 wt % UF_4 hydrates (Figure S34). This result likely overestimates the fraction of UF_4, $UF_4{\cdot}1.2H_2O$, and $UF_4{\cdot}1.5H_2O$ because other phases in the sample were not accounted for. Based on the observation for the UF_4 aged at 293 K and 95% RH, it is expected that additional aging time would further increase the concentration of UF_4 hydrates for the sample aged at 308 K and 91%

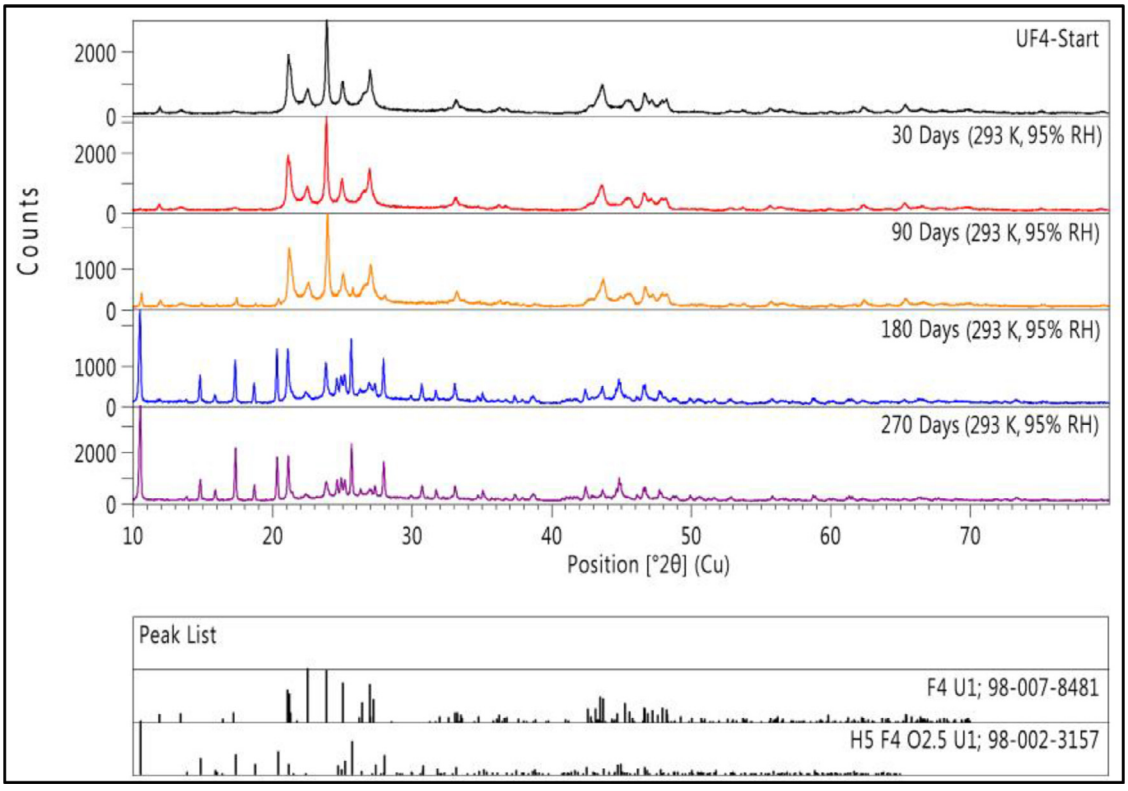

Fig. 1. Powder-XRD patterns for UF_4 after 0 (black), 30 (red), 90 (orange), 180 (blue), and 270 (purple) days aging at 293 K and 95% RH. The material began as UF_4 and was converted into a mixture of UF_4 (PDF #98-007-8481) and $UF_4{\cdot}2.5H_2O$ (PDF #98-002-3157).

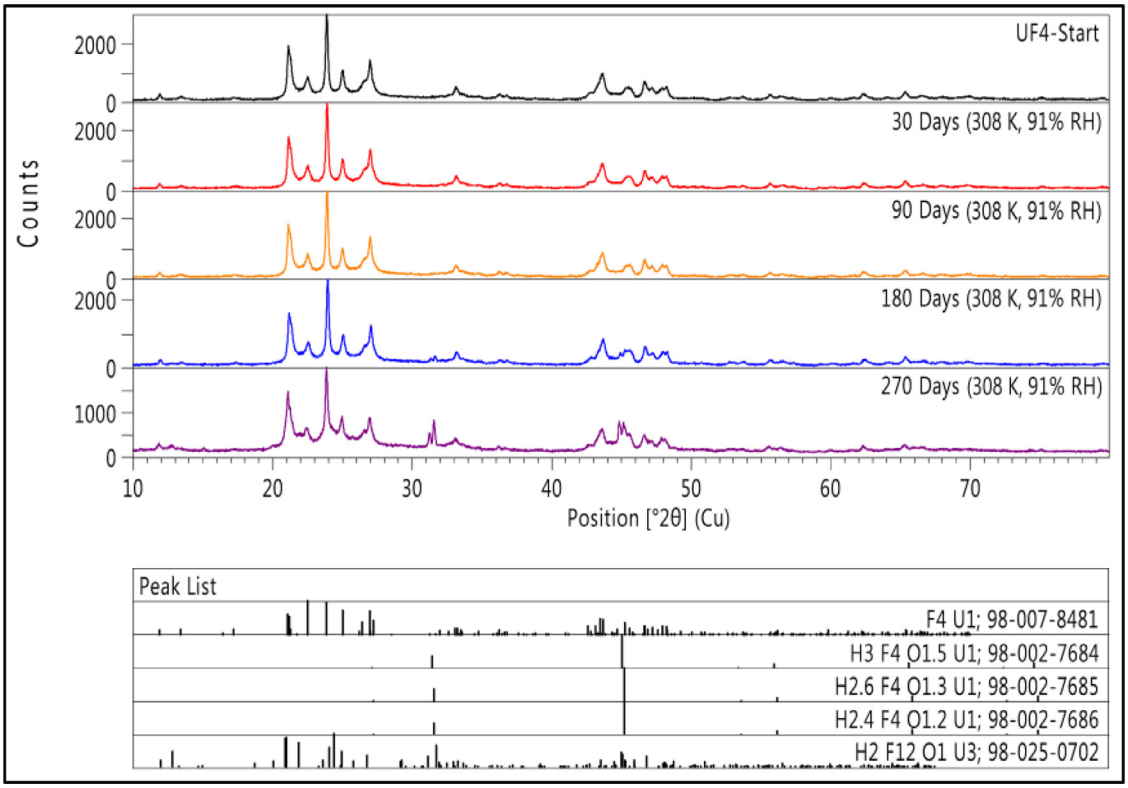

Fig. 2. Powder-XRD patterns for UF_4 after 0 (black), 30 (red), 90 (orange), 180 (blue), and 270 (purple) days aging at 308 K and 91% RH. The material began as UF_4 and was converted into a mixture of UF_4 (PDF #98-007-8481) and one or more UF_4 hydrates. The possible UF_4 hydrates are $UF_4{\cdot}1.5H_2O$ (PDF #98-002-7684), $UF_4{\cdot}1.3H_2O$ (PDF #98-002-7685), $UF_4{\cdot}1.2H_2O$ (PDF #98-002-7686), and $U_3F_{12}{\cdot}H_2O$ (PDF #98-025-0702).

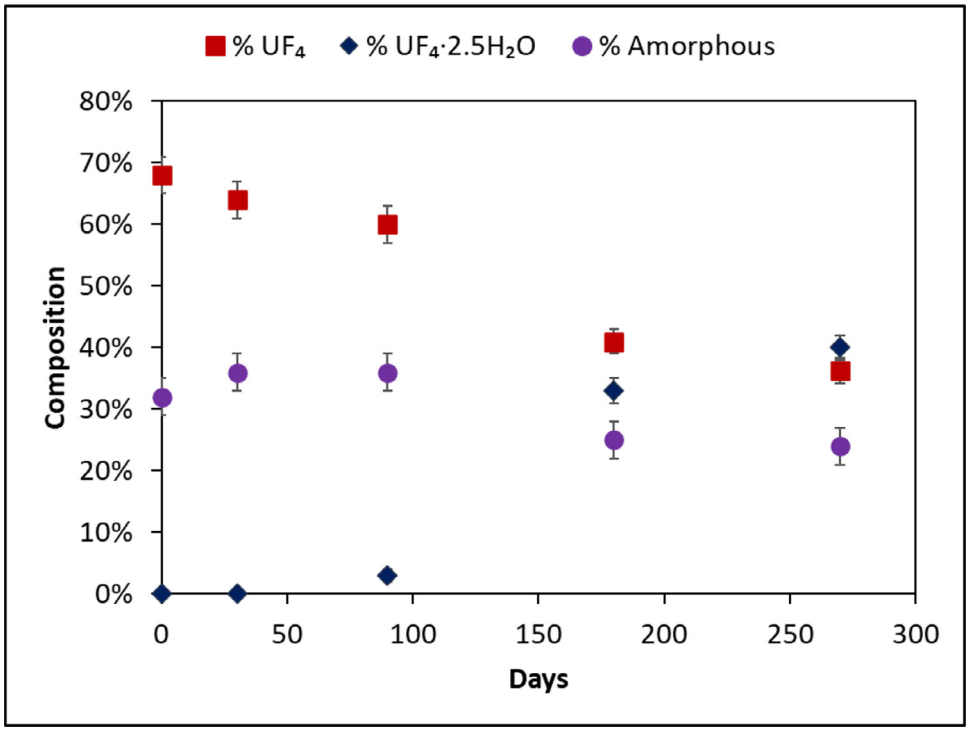

Fig. 3. QPA results for UF_4 after 0, 30, 90, 180, and 270 days aging at 293 K and 95% RH. Uncertainties are 1σ.

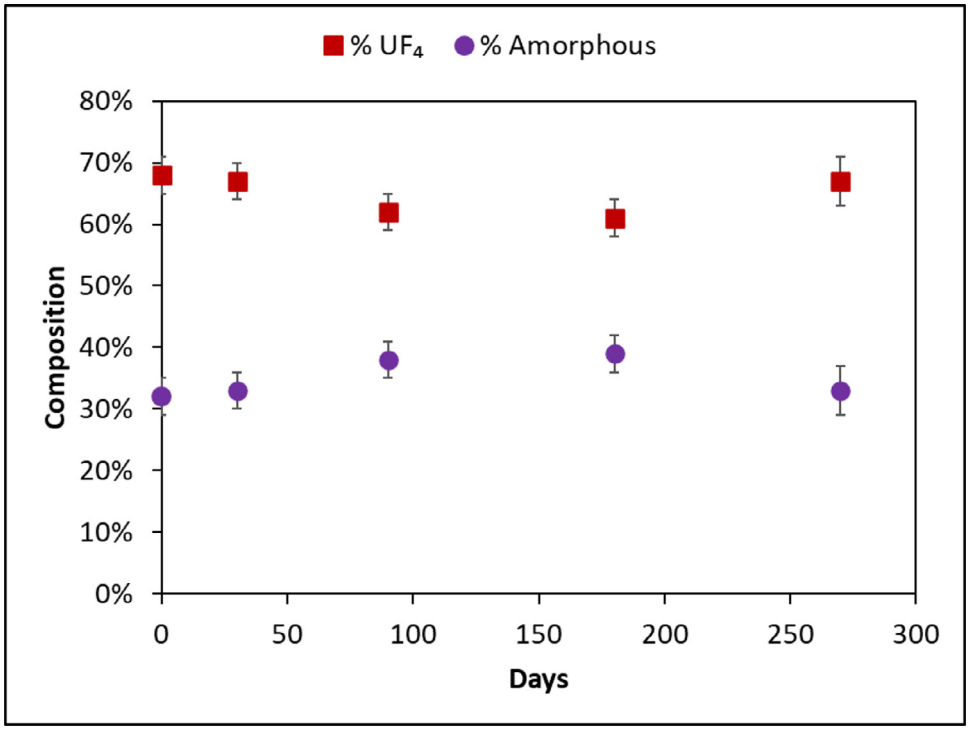

Fig. 4. QPA results for UF_4 after 0, 30, 90, 180, and 270 days aging at 308 K and 32% RH. Uncertainties are 1σ.

RH. Furthermore, Dawson et al. reported $UF_4{\cdot}2.5H_2O$ can be prepared by suspending the lower hydrates of UF_4 in dilute hydrofluoric acid [38]. Given that Christian et al. prepared $UF_4{\cdot}2.5H_2O$ from UF_4 in neat water instead of dilute hydrofluoric acid, it is plausible, but unknown, whether $UF_4{\cdot}2.5H_2O$ would be formed in this sample with additional aging time.

The QPA results for the remaining storage conditions initially indicated that exposure to the various conditions increased the fraction of amorphous content in the samples. For example, the amorphous content of the sample aged at 308 K and 32% RH increased from approximately 32% to 39% during the first 180 days of aging (Fig. 4). However, the 270-day QPA results did not fall within the tentative trend, indicating the trend did not exist and the variations in the amorphous fraction likely arise from uncertainty in the QPA results. Thus, the QPA results for the lower RH (<90%) conditions indicated those samples remained unchanged

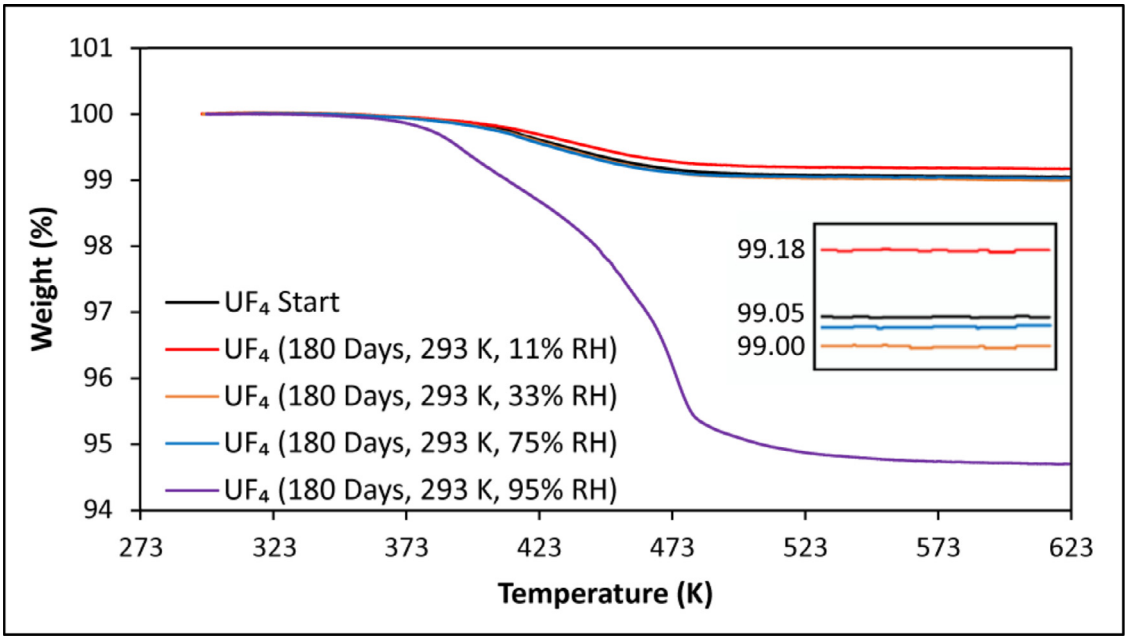

Fig. 5. TGA results for UF_4 starting material (black) and UF_4 aged for 180 days at 293 K and 11% (red), 33% (orange), 75% (blue), or 95% (purple) RH. The inset is a magnified view for 613 - 623 K.

during the aging study, consistent with the qualitative pXRD observations.

Following 180 days aging, a sub-set of the UF_4 samples were analyzed via TGA to determine whether the changes in amorphous content, indicated by QPA at that time, arose from partial hydration of the UF_4. Results from TGA analysis of the samples aged at 293 K and the various RH conditions are shown in Fig. 5. Consistent with the pXRD data for the sample aged at 95% RH, the TGA results show loss of water beginning around 363 K. The 5.3% wt loss observed would equate to a material that is approximately 42% $UF_4{\cdot}2.5H_2O$, based on the theoretical mass loss for complete dehydration of $UF_4{\cdot}2.5H_2O$ (*calc. 12.5% wt loss*). Given that some of the mass loss could arise from absorbed but non-crystalline water in the sample, this result shows good agreement with the QPA results, but the final product composition is not known with certainty. However, because the TGA was performed under an argon flow and the maximum temperature was 623 K, above which it has been shown UF_4 undergoes pyrohydrolysis, oxidation is unlikely to occur [39]. The final product is likely UF_4 or a mixture of UF_4 and a fractional hydrate, potentially $UF_4{\cdot}0.1H_2O$. Perhaps more interesting are the TGA results for the UF_4 starting material and other relative humidity conditions. The UF_4 staring material shows a small mass loss of approximately 1%, indicating the starting material contains a fraction of UF_4 hydrate. Though not known with certainty, this hydrate could explain the amorphous phase present in the pXRD data for the UF_4 starting material. If this correct, based on the fraction of amorphous phase (~30%) and the total mass loss observed in the TGA results (1%), the amorphous phase would be approximately $UF_4{\cdot}0.5H_2O$. For the samples aged at 33 and 75% RH, there is essentially no difference in the TGA curves compared to the UF_4 starting material, indicating additional hydration had not occurred to the UF_4 stored under these conditions. However, for the sample aged at 11% RH, the TGA curve displayed slightly less mass loss than the UF_4 starting material, 0.8% and 1.0% respectively, indicating storage in low relative humidity slightly *dehydrated* the UF_4.

Overall, the combined qualitative and quantitative results indicate the interaction of UF_4 with various environmental conditions is complex, especially considering the studies by Wellons et al. and Pointurier et al. investigating UF_4 particulate matter. Consistent with the conventional understanding that UF_4 is stable under ambient conditions, this study indicates that bulk UF_4 is stable for up to 9 months exposure to moderate and warm temperatures (293 and 308 K) and low to moderately high relative humidity (≤75% RH), as no changes in chemical speciation were observed for samples aged under those conditions. However, the observations for samples exposed to high relative humidity (>90% RH) depart from the conventional understanding of UF_4 stability. Exposure to 95% RH at 293 K resulted in the formation of $UF_4{\cdot}2.5H_2O$ within 30 days. Additional aging time resulted in increasing concentrations of $UF_4{\cdot}2.5H_2O$. Increasing the temperature to 308 K yielded a different outcome, where changes in chemical speciation were delayed by several months and the resulting compound(s) were UF_4 hydrates with less than 2.5 waters of hydration. This may be explained by multiple factors. First, the thermodynamic data [40] indicates the reaction forming $UF_4{\cdot}2.5H_2O$ (Eq 3) is entropically disfavored where ΔS° = -360 J K^{-1} mol^{-1} (Table 2). Second, changes in temperature affect water sorption, where, in general, the amount of water absorbed by a material decreases with increasing temperature [41–43]. Reducing the water absorbed by UF_4 could slow the formation of UF_4 hydrates and also limit the available water resulting in the formation of hydrates containing less than 2.5 waters of hydration.

$$UF_4(s) + 2.5H_2O(g) \rightarrow UF_4 \cdot 2.5H_2O(s) \quad (3)$$

Additionally, the qualitative and quantitative results indicate there exists a threshold RH below which there is insufficient water vapor present for UF_4 to hydrate, or UF_4 hydrates so slowly that no changes were evident following 9 months exposure. A similar observation was reported by Tamasi et al.; they found U_3O_8 exposed to low RH (≤25%) for up to 3.5 years remained unchanged whereas U_3O_8 exposed to high RH (≥89%) for up to 3.5 years exhibited changes in chemical speciation due to oxidation and hydration [21]. This phenomenon has also been observed for the hydration of other inorganic salts [44–46].

From a thermodynamic perspective the hydration of a salt is characterized by Gibbs free energy at standard conditions (Eq 4) where ΔH° ($J{\cdot}mol^{-1}$) and ΔS° ($J{\cdot}K^{-1}{\cdot}mol^{-1}$) are the reaction en-

Table 2
Thermodynamic data for reaction forming $UF_4{\cdot}2.5H_2O$ [40].

	$\Delta G_f°$ (kJ·mol^{-1})	$\Delta H_f°$ (kJ·mol^{-1})	S° (J·K^{-1}·mol^{-1})
UF_4(s)	-1823.5 ± 4.2	-1914.2 ± 4.2	151.7 ± 0.2
H_2O(g)	-228.58 ± 0.04	-241.83 ± 0.04	188.84 ± 0.01
$UF_4{\cdot}2.5H_2O$(s)	-2440.3 ± 6.2	-2671.5 ± 4.3	263.5 ± 15.0
	$\Delta G°$ (kJ·mol^{-1})	$\Delta H°$ (kJ·mol^{-1})	$\Delta S°$ (J·K^{-1}·mol^{-1})
Overall reaction (298 K)	-45.3 ± 7.5	-152.7 ± 6.0	-360 ± 15

Table 3
Thermodynamic equilibrium data for reaction forming $UF_4{\cdot}2.5H_2O$ at 298 K.

Uncertainty Range ($\Delta G°$)	$\Delta G°$ (kJ·mol^{-1})	ρ_{eq} [kPa (atm)]	RH (%)
Min. -45.3 - 7.5	-52.8	0.020 (2.0 × 10^{-4})	0.64
-45.3	-45.3	0.068 (6.7 × 10^{-4})	2.1
Max. -45.3 + 7.5	-37.8	0.23 (2.2 × 10^{-3})	7.2

Table 4
Relative quantification of fluorine and oxygen for the surface of UF_4 and UO_2F_2 via XPS. Uncertainties are 1σ.

Ratio	UF_4 Start	UO_2F_2
U/F	4.6 ± 0.1	7.3 ± 0.2
U/O	51 ± 5	10 ± 2

thalpy and entropy, T (K) is absolute temperature, R (J·K^{-1}·mol^{-1}) is the gas constant, ρ_{eq} (kPa or atm) is the water vapor pressure in equilibrium with the salt, ρ^0 is standard pressure (101.3 kPa or 1 atm), and n is the number of moles of water for the reaction. By rearranging Eq 4, ρ_{eq} can be calculated from the standard Gibbs free energy of reaction for Eq 3, ΔG^o = -43.5 ± 7.5 kJ mol^{-1}. Using the saturated water vapor pressure at 298 K (3.16 kPa or 0.0312 atm) and calculated range of values for ρ_{eq}, the RH at thermodynamic equilibrium for $UF_4{\cdot}2.5H_2O$ is shown in Table 3. Based on this range of RH at thermodynamic equilibrium (RH = $2.1^{+5.1}_{-1.5}$ %), the formation $UF_4{\cdot}2.5H_2O$ from UF_4 is thermodynamically favorable at RH greater than 7.2%. Our observation that much higher RH conditions are necessary to form $UF_4{\cdot}2.5H_2O$ suggests the reaction is significantly hindered kinetically, and the threshold RH required to overcome this kinetic barrier appears to lie between 75 and 95% but is not known with certainty. Studies incorporating longer aging times and investigations of additional RH conditions between 75 and 90% are needed to resolve this uncertainty.

$$\Delta G^\circ = \Delta H^\circ - T\Delta S^\circ = RT\ln\left[\left(\frac{\rho_{eq}}{\rho^0}\right)^n\right] \quad (4)$$

Lastly, the qualitative and quantitative observations demonstrate chemical changes to bulk UF_4 may occur under certain temperature and relative humidity conditions. Until recently, $UF_4{\cdot}2.5H_2O$, the highest established UF_4 hydrate, had only been prepared by reacting anhydrous UF_4 with hydrofluoric acid, however Christian et al. demonstrated it could be formed by reacting UF_4 with neat liquid water at room temperature [38,47]. Our findings represent the first report of UF_4 hydrates formed via a room temperature reaction between UF_4 and atmospheric water vapor.

3.3. XPS analysis of UF_4 and aged UF_4 samples

A sub-set of the UF_4 samples were analyzed via XPS to determine whether the UF_4 surface underwent degradation consistent with the observations of Wellons et al. and Pointurier et al., or hydration as observed for the bulk UF_4. Recently, Giannuzzi et al. analyzed UF_4 particles using scanning transmission electron microscopy coupled to electron energy loss spectroscopy (STEM/EELS) and reported reduced fluorine content at the particle edges compared to the bulk material, indicating surface limited reactions had occurred [48]. This observation demonstrates the importance of characterizing the surface of the aged UF_4 sample. The probing depth for XPS measurements is generally accepted to be 3 – 10 nm, making it a suitable technique to investigate changes to the surface of the UF_4 [49]. Conversion of UF_4 to $UO_2F_2{\cdot}2H_2O$ and then UOCs such as $UO_3{\cdot}xH_2O$ or $UO_2(O_2){\cdot}xH_2O$ requires significant chemical transformations including fluoride ligand substitution, oxo bond formation, and uranium oxidation [28,29]. These changes in chemical speciation would be evident in XPS spectra via fluorine signal loss, oxygen signal gain, and changes to features of the U 4f core-level spectra.

The XPS spectra for the as-received UF_4 and synthesized UO_2F_2, the first product of the degradation pathways reported by Wellons et al., were collected to obtain references that would help assign potential differences expected if the UF_4 surface degrades with formation of UO_2F_2 (Fig. 6). The UF_4 and UO_2F_2 XPS spectra collected for this study were consistent with previously published spectra [50–52]. The XPS spectrum of as-received UF_4 shows a small oxygen signal which could be attributed to several possible sources. It is well established that adventitious carbon containing oxygen, adsorbed gases (CO_2, O_2, H_2O), or other minor contaminants can contribute to the oxygen signal [49,53]. It is also possible the as-received UF_4 contains a very small amount of the UO_2 starting material from which it was prepared. However, the lack of distinguishable features in the U 4f core-level spectrum suggests only a very small amount of UO_2 may be present. The increase in oxygen signal between UF_4 and UO_2F_2 is apparent in the XPS survey spectra and also is shown in relative quantification of the oxygen content, indicated by the decrease in the U/O ratio (Table 4). For all relative quantification in this work, the convention used to calculate the ratios, U/O or U/F, will result in a decrease in the ratio as oxygen or fluorine content increases. The expected change in the fluorine signal is also immediately discernable in the survey spectra, and relative quantification of the fluorine content from the F 1s signal shows a decrease in fluorine, indicated by the increase in the U/F ratio. For the U 4f core-level spectra, two changes are notable; first there is a shift to slightly higher binding energy (BE), from 382.6 to 382.8 eV for the U $4f_{7/2}$ peaks. Second, the UF_4 spectrum clearly exhibits a satellite structure common to several U(IV) compounds at a position that is 7.0 eV higher BE than the U 4f peaks. Conversely, this satellite structure is absent for UO_2F_2. In fact, the UO_2F_2 does not readily exhibit any satellite structures though several other U(VI) compounds do [51,52].

Pure samples of metaschoepite (abbreviated as $UO_3{\cdot}2H_2O$) and uranyl peroxide [$UO_2(O_2){\cdot}2H_2O$], degradation products identified by both Wellons et al. and Pointurier et al., were not available for this study. For $UO_3{\cdot}2H_2O$, the literature reports the U $4f_{7/2}$ at BE of 382.0 eV and indicates that the U 4f core-level spectrum does not readily exhibit a satellite structure [54,55]. For $UO_2(O_2){\cdot}2H_2O$, the literature reports the BE of U $4f_{7/2}$ BE at 382.3 eV and demonstrates the presence of a small satellite structure at 3.5 eV higher BE than the primary U 4f peaks [56]. Overall, degradation of the UF_4 surface consistent with the pathways reported by Wellons et al. and Pointurier et al. would be evident by a loss of fluorine,

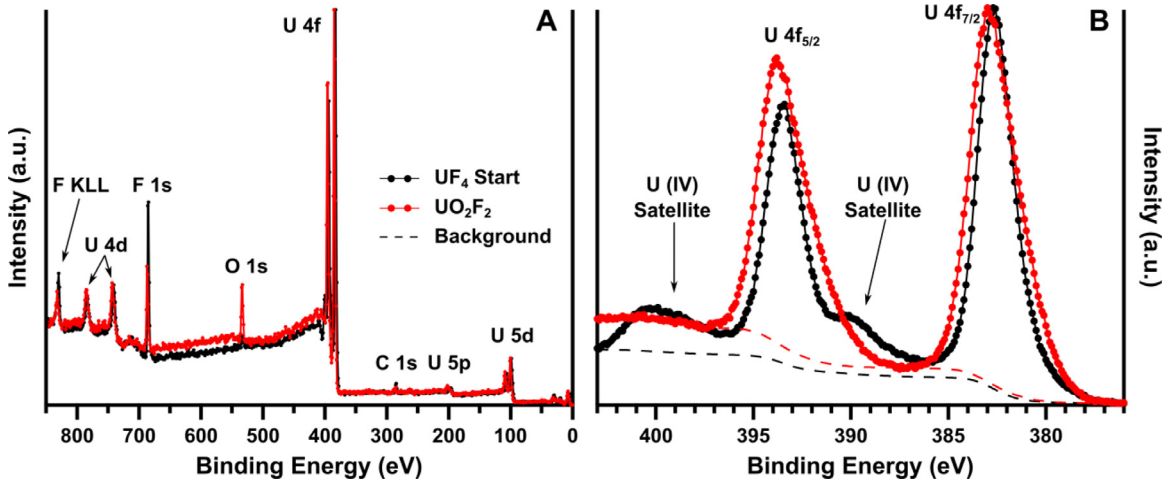

Fig. 6. XPS survey spectra (A) and U 4f core-level spectra (B) for as-received UF_4 (black) and synthesized UO_2F_2 (red). Spectra are displayed with normalization applied by scaling to the maximum and minimum points of the spectra to clearly show relative changes in spectral features.

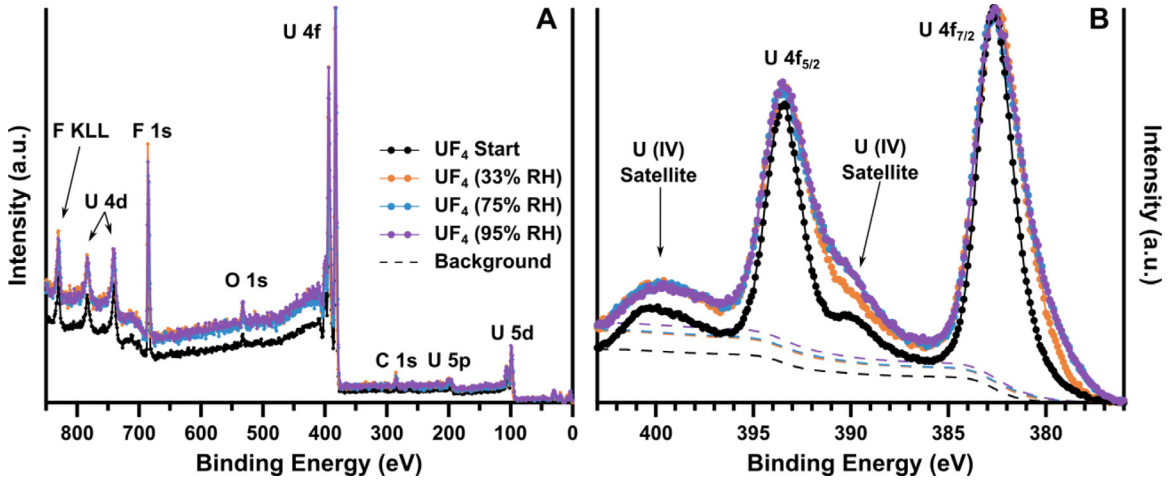

Fig. 7. XPS survey spectra (A) and U 4f core-level spectra (B) for as-received UF_4 (black) and UF_4 aged for 180 days at 293 K and 95% (purple), 75% (blue), or 33% (orange) RH. Spectra are displayed with normalization applied by scaling to the maximum and minimum points of the spectra to clearly show relative changes in spectral features.

an increase in oxygen, shifts in the U 4f BEs, and a loss or shift in the U 4f satellite structure.

The XPS spectra for the UF_4 starting material and the subset of aged UF_4 samples analyzed are shown in Fig. 7. The survey spectra for all the samples are remarkably similar. Relative quantification indicated the fluorine content remained unchanged for the UF_4 stored for 180 days at 293 K and 33% RH and the UF_4 stored for 180 days at 293 K and 75% RH (Table 5). However, relative quantification indicated a small amount of fluorine loss (~15 % change) for the UF_4 stored for 180 days at 293 K and 95% RH, which exhibited the largest changes in the pXRD and TGA data. However, the difference in the U/F ratio is much less than that observed between UF_4 and UO_2F_2. Interestingly, relative quantification of the oxygen content reveals successive increases in oxygen content across the samples that parallels increases in the RH aging conditions. However, similar to the U/F ratio, the greatest change in the U/O ratio is much less than what is expected if UF_4 was converted to UO_2F_2. The U 4f core-level spectra for each aged sample shows a slight shift to lower BE for the U 4f peaks as well as slight broadening toward lower BE, indicating the presence of another uranium species. However, a shift to lower BE is not consistent with the formation of UO_2F_2, additionally, the U 4f core-level spectrum of each aged sample still exhibits the U(IV) satellite structure, which should decrease or be absent if a significant fraction of the UF_4 surface had oxidized to UO_2F_2, $UO_3{\cdot}2H_2O$, or $UO_2(O_2){\cdot}2H_2O$.

Overall, the XPS data for the aged UF_4 samples suggests the UF_4 surface has undergone hydration. The stepwise increase in oxygen content with respect to increasing RH, combined with a lack of corresponding fluorine loss would be consistent with UF_4 hydrate formation on the surface. Additionally, the continued presence of the U(IV) satellite feature indicates the uranium in the aged samples remained in the U(IV) oxidation state. The slight shift to lower BEs accompanied by the broadening of the primary peaks in the U 4f core-level spectra could also be consistent with the hypothesis of

Table 5
Relative quantification of fluorine and oxygen for the surface of unaged and aged UF_4 via XPS. Uncertainties are 1σ.

Ratio	UF_4 Start	UF_4 (180 days, 293 K, 33% RH)	UF_4 (180 days, 293 K, 75% RH)	UF_4 (180 days, 293 K, 95% RH)
U/F	4.6 ± 0.1	4.5 ± 0.2	4.4 ± 0.2	5.3 ± 0.2
U/O	51 ± 5	40 ± 2	37 ± 2	30 ± 2

UF_4 hydrate formation. The uranium atoms in UF_4 are coordinated to 8 fluoride ligands whereas $UF_4{\cdot}2.5H_2O$ displays two uranium environments; one in which the uranium atoms are either coordinated to 9 fluoride ligands or coordinated to 5 fluoride ligands and 4 water ligands [57,58]. The change in uranium coordination environment from only fluoride ligands to a combination of fluoride and water ligands could result in a shift of the U 4f core-level peaks to lower BE as water is less electronegative than fluorine, reducing the effective nuclear charge experienced by the uranium electrons. Unfortunately, reference XPS spectra for UF_4 hydrates are not available, precluding a direct comparison with the results of this study.

In summary, the results from the XPS data are largely consistent with our observations for the aged bulk UF_4 studied by XPS and TGA. For the sample stored at 95% RH, both surface and bulk analysis indicate UF_4 hydrate formation had occurred. For the samples stored at 33 and 75% RH, the XPS results suggest slight hydration of the surface occurred, but the extent of hydration remained below pXRD detection limits. The exception to these observations is the small amount of surface fluorine loss for the sample stored in 95% RH, however the resulting surface uranium species is unknown at this time. Finally, the XPS data showing an incremental increase in surface degradation with respect to increasing RH supports the idea that the formation of UF_4 hydrates under these various conditions is thermodynamically favorable but significantly hindered kinetically. Thus, at lower RH ($\leq$75 %), hydration of the bulk material may eventually occur with considerably longer aging times.

4. Conclusions

The potential impact to nuclear forensics, nuclear nonproliferation efforts, and the nuclear industry drives an ongoing need to study the physical and chemical characteristics of nuclear fuel cycle materials, including the chemical and physical changes that may occur in nuclear materials during periods of storage. For this study, chemical transformations of UF_4 were investigated by aging anhydrous UF_4 under various temperature and RH conditions. Using pXRD and TGA, bulk UF_4 was found to remain unchanged when aged at low to moderately high ($\leq$75%) RH and 293 or 308 K for up to 9 months, however, exposure to high relative humidity led to the formation of UF_4 hydrates. Specifically, $UF_4{\cdot}2.5H_2O$ was formed within 30 days for UF_4 aged at 293 K and 95% RH, and UF_4 hydrates with less than 2.5 waters of hydration were formed by 180 days for UF_4 aged at 308 K and 91% RH. XPS analysis indicated changes in chemical speciation to the UF_4 surface were likely UF_4 hydration as well, as opposed to formation of UO_2F_2.

For the nuclear industry, these results, combined with the observations of Christian et al., indicate anhydrous UF_4 can be preserved by protecting it from high RH and direct exposure to liquid water during storage [47]. For nuclear forensics and nuclear nonproliferation efforts, this work indicates UF_4 may persist in the environment for up to several months, preserving a valuable signature of anthropogenic nuclear activity. Additionally, $UF_4{\cdot}2.5H_2O$ may serve as an indicator of UF_4 exposed to or stored in high RH conditions. This work demonstrates the value and necessity of using multi-technique characterization, including both bulk and surface chemical analysis, for nuclear forensics investigations because important signatures or indicators may be exclusive to one of these domains. It is noteworthy that one environmental condition, UV light exposure, was not investigated in this study as the aging containers were protected from light. UV light has been demonstrated to play a role in altering the chemical speciation of uranium compounds and thus, UV light exposure could affect the chemical changes in bulk UF_4 [28,59]. Future work will investigate longer aging times and additional RH points between 75 and 95% to determine whether a threshold RH exists, below which no hydration will occur within several years. Future work will also investigate the effect of UV light exposure on the chemical transformations of bulk UF_4. Lastly, producing high quality samples for reference XPS spectra is challenging, however acquiring a reference XPS spectrum for $UF_4{\cdot}2.5H_2O$ and lesser UF_4 hydrates is also of interest for future work.

Declaration of Competing Interest

The authors declare that they have no known competing financial interests or personal relationships that could have appeared to influence the work reported in this paper.

CRediT authorship contribution statement

Kevin J. Pastoor: Conceptualization, Investigation, Formal analysis, Visualization, Writing – original draft. **Michael J. Dzara:** Investigation, Formal analysis, Visualization, Writing – review & editing. **Svitlana Pylypenko:** Conceptualization, Supervision, Writing – review & editing. **Jenifer C. Shafer:** Conceptualization, Supervision, Funding acquisition, Project administration, Writing – review & editing. **Mark P. Jensen:** Conceptualization, Supervision, Funding acquisition, Project administration, Writing – review & editing.

Acknowledgments

K.J.P. and J.C.S. acknowledge support from DTRA grant #HDTRA1-18-1-0015. We thank the Toberer Group at the Colorado School of Mines for training and use of the pXRD instrument. This work makes use of the E-XPS system at the Colorado School of Mines, which was supported by the National Science Foundation under Grant No. 1626619. The views and conclusions expressed in this document are those of the authors and do not reflect the official policy or position of the United States Air Force, Department of Defense, or the U.S. Government.

Supplementary materials

Supplementary material associated with this article can be found, in the online version, at doi:10.1016/j.jnucmat.2021.153260.

References

[1] IAEA, Development and implementation support programme for nuclear verification 2020–2021, IAEA, Vienna, Austria (2020).
[2] K. Mayer, Expand nuclear forensics, Nature 503 (7477) (2013) 461–462.
[3] K.J. Pastoor, R.S. Kemp, M.P. Jensen, J.C. Shafer, Progress in uranium chemistry: driving advances in front-end nuclear fuel cycle forensics, Inorg. Chem. 60 (12) (2021) 8347–8367.
[4] J. Svedkauskaite-LeGore, K. Mayer, S. Millet, A. Nicholl, G. Rasmussen, D. Baltrunas, Investigation of the isotopic composition of lead and of trace elements concentrations in natural uranium materials as a signature in nuclear forensics, Radiochim. Acta 95 (10) (2007) 601–605.
[5] Z. Varga, M. Wallenius, K. Mayer, E. Keegan, S. Millett, Application of lead and strontium isotope ratio measurements for the origin assessment of uranium ore concentrates, Anal. Chem. 81 (20) (2009) 8327–8334.
[6] V. Migeon, C. Fitoussi, E. Pili, B. Bourdon, Molybdenum isotope fractionation in uranium oxides and during key processes of the nuclear fuel cycle: towards a new nuclear forensic tool, Geochim. Cosmochim. Acta 279 (2020) 238–257.
[7] J. Krajko, Z. Varga, E. Yalcintas, M. Wallenius, K. Mayer, Application of neodymium isotope ratio measurements for the origin assessment of uranium Ore concentrates, Talanta 129 (2014) 499–504.
[8] Q.R. Shollenberger, L.E. Borg, E.C. Ramon, M.A. Sharp, G.A. Brennecka, Samarium isotope compositions of uranium ore concentrates: a novel nuclear forensic signature, Talanta 221 (2021) 121431.
[9] Z. Varga, M. Wallenius, K. Mayer, Origin assessment of Uranium Ore Concentrates based on their rare-earth elemental impurity pattern, Radiochim. Acta 98 (12) (2010) 771–778.
[10] E. Keegan, M. Wallenius, K. Mayer, Z. Varga, G. Rasmussen, Attribution of Uranium Ore concentrates using elemental and anionic data, Appl. Geochem. 27 (8) (2012) 1600–1609.

[11] E. Balboni, N. Jones, T. Spano, A. Simonetti, P.C. Burns, Chemical and Sr isotopic characterization of North America Uranium Ores: nuclear forensic applications, Appl. Geochem. 74 (2016) 24–32.
[12] A.J. Fahey, N.W.M. Ritchie, D.E. Newbury, J.A. Small, The use of lead isotopic abundances in trace uranium samples for nuclear forensics analysis, J. Radioanal. Nucl. Chem. 284 (3) (2010) 575–581.
[13] T.L. Spano, A. Simonetti, E. Balboni, C. Dorais, P.C. Burns, Trace Element and U Isotope Analysis of Uraninite and Ore Concentrate: Applications for Nuclear Forensic Investigations, Appl. Geochem. 84 (2017) 277–285.
[14] T.L. Spano, A. Simonetti, T. Wheeler, G. Carpenter, D. Freet, E. Balboni, C. Dorais, P.C. Burns, A novel nuclear forensic tool involving deposit type normalized rare earth element signatures, Terra Nova 29 (5) (2017) 294–305.
[15] A.L. Tamasi, L.J. Cash, W.T. Mullen, A.R. Ross, C.E. Ruggiero, B.L. Scott, G.L. Wagner, J.R. Walensky, S.A. Zerkle, M.P. Wilkerson, Comparison of morphologies of a Uranyl peroxide precursor and calcination products, J. Radioanal. Nucl. Chem. 309 (2) (2016) 827–832.
[16] A.M. Olsen, B. Richards, I. Schwerdt, S. Heffernan, R. Lusk, B. Smith, E. Jurrus, C. Ruggiero, L.W. McDonald, Quantifying morphological features of α-U_3O_8 with image analysis for nuclear forensics, Anal. Chem. 89 (5) (2017) 3177–3183.
[17] I.J. Schwerdt, A. Olsen, R. Lusk, S. Heffernan, M. Klosterman, B. Collins, S. Martinson, T. Kirkham, L.W. McDonald, Nuclear forensics investigation of morphological signatures in the thermal decomposition of uranyl peroxide, Talanta 176 (2018) 284–292.
[18] E.C. Abbott, A. Brenkmann, C. Galbraith, J. Ong, I.J. Schwerdt, B.D. Albrecht, T. Tasdizen, L.W. McDonald, Dependence of UO_2 surface morphology on processing history within a single synthetic route, Radiochim. Acta 107 (12) (2019) 1121–1131.
[19] I.J. Schwerdt, C.G. Hawkins, B. Taylor, A. Brenkmann, S. Martinson, L.W. McDonald, Uranium oxide synthetic pathway discernment through thermal decomposition and morphological analysis, Radiochim. Acta 107 (3) (2019) 193–205.
[20] C.A. Nizinski, A.B. Hanson, B.C. Fullmer, N.J. Mecham, T. Tasdizen, L.W. McDonald, Effects of process history on the surface morphology of uranium ore concentrates extracted from Ore, Miner. Eng. 156 (2020) 106457.
[21] A.L. Tamasi, K.S. Boland, K. Czerwinski, J.K. Ellis, S.A. Kozimor, R.L. Martin, A.L. Pugmire, D. Reilly, B.L. Scott, A.D. Sutton, G.L. Wagner, J.R. Walensky, M.P. Wilkerson, Oxidation and hydration of U_3O_8 materials following controlled exposure to temperature and humidity, Anal. Chem. 87 (8) (2015) 4210–4217.
[22] S.B. Donald, Z.R.R. Dai, M.L. Davisson, J.R. Jeffries, A.J. Nelson, An XPS study on the impact of relative humidity on the aging of UO_2 powders, J. Nucl. Mater. 487 (2017) 105–112.
[23] A.L. Tamasi, L.J. Cash, W.T. Mullen, A.L. Pugmire, A.R. Ross, C.E. Ruggiero, B.L. Scott, G.L. Wagner, J.R. Walensky, M.P. Wilkerson, Morphology of U_3O_8 materials following storage under controlled conditions of temperature and relative humidity, J. Radioanal. Nucl. Chem. 311 (1) (2017) 35–42.
[24] M.P. Wilkerson, S.C. Hernandez, W.T. Mullen, A.T. Nelson, A.L. Pugmire, B.L. Scott, E.S. Sooby, A.L. Tamasi, G.L. Wagner, J.R. Walensky, Hydration of α-UO_3 following storage under controlled conditions of temperature and relative humidity, Dalton Trans. 49 (30) (2020) 10452–10462.
[25] A.B. Hanson, I.J. Schwerdt, C.A. Nizinski, R.N. Lee, N.J. Mecham, E.C. Abbott, S. Heffernan, A.M. Olsen, M.R. Klosterman, S. Martinson, A. Brenkmann, L.W. McDonald, Impact of controlled storage conditions on the hydrolysis and surface morphology of amorphous-UO_3, ACS Omega 6 (12) (2021) 8605–8615.
[26] M.C. Kirkegaard, M.W. Ambrogio, A. Miskowiec, A.E. Shields, J.L. Niedziela, T.L. Spano, B.B. Anderson, Characterizing the degradation of $[(UO_2F_2)(H_2O)]_7{\cdot}4H_2O$ under humid conditions, J. Nucl. Mater. 529 (2020) 151889.
[27] K.J. Pastoor, S.L. Robinson, R.A. Greenwell, C.V. Quintero Hilsaca, J.C. Shafer, M.P. Jensen, Understanding uranium oxide hardening during prolonged storage, Radiochim. Acta 108 (12) (2020) 943–953.
[28] F. Pointurier, C. Lelong, O. Marie, Study of the chemical changes of μm-sized particles of uranium tetrafluoride (UF_4) in environmental conditions by means of micro-Raman spectrometry, Vib. Spectrosc. 110 (2020) 103145.
[29] M. Wellons, M. DeVore, E. Villa-Aleman, M. Summer, R. Smith, C. Klug, T. Daroudi, Characterization of the environmentally induced chemical transformations of uranium tetrafluoride, SRNL-MS-2017-00048, Savannah River National Laboratory, SC (2017) 101–106.
[30] J.J. Katz, E. Rabinowitch, Nonvolatile fluorides of uranium, in: The Chemistry of Uranium: The Element, its Binary and Related Compounds, Dover Publications, Inc., New York, NY, 1961, pp. 349–395.
[31] M.C. Chakravorti, M. Chowdhury, P.G. Eller, R.J. Kissane, Difluorodioxouranium(VI), Inorg. Synth. 25 (1989) 144–146.
[32] L. Greenspan, Humidity fixed-points of binary saturated aqueous-solutions, J. Res. Natl. Bur. Stand. 81 (1) (1977) 89–96.
[33] T. Degen, M. Sadki, E. Bron, U. König, G. Nénert, The HighScore suite, Powder Diffr. 29 (S2) (2014) S13–S18.
[34] S. Gates-Rector, T. Blanton, The powder diffraction file: a quality materials characterization database, Powder Diffr. 34 (4) (2019) 352–360.
[35] I.C. Madsen, N.V.Y. Scarlett, A. Kern, Description and survey of methodologies for the determination of amorphous content via X-ray powder diffraction, Z. Kristallogr. - Cryst. Mater. 226 (12) (2011) 944–955.
[36] L.B. McCusker, R.B. Von Dreele, D.E. Cox, D. Louer, P. Scardi, Rietveld refinement guidelines, J. Appl. Crystallogr. 32 (1999) 36–50.
[37] R. Snellings, L. Machiels, G. Mertens, J. Elsen, Rietveld refinement strategy for quantitative phase analysis of partially amorphous Zeolitized Tuffaceous rocks, Geol. Belg. 13 (3) (2010) 183–195.
[38] J.K. Dawson, R.W.M. D'Eye, A.E. Truswell, The hydrated tetrafluorides of uranium and plutonium, J. Chem. Soc. (1954) 3922–3929.
[39] M. Iwasaki, N. Ishikawa, Pyrohydrolysis reactions of UF_4 and UO_2F_2 - effect of oxygen on reactions, J. Nucl. Sci. Technol. 20 (5) (1983) 400–404.
[40] R. Guillaumont, T. Fanghanel, V. Neck, J. Fuger, D.A. Palmer, I. Grenthe, M.H. Rand, Chemical Thermodynamics Vol. 5: Update on the Chemical Thermodynamics of Uranium, Neptunium, Plutonium, Americium, and Technetium, Elsevier, Issy-les-Moulineaux, 2003.
[41] S. Brunauer, P.H. Emmett, E. Teller, Adsorption of gases in multimolecular layers, J. Am. Chem. Soc. 60 (1938) 309–319.
[42] S. Brunauer, L.S. Deming, W.E. Deming, E. Teller, On a theory of the van der waals adsorption of gases, J. Am. Chem. Soc. 62 (1940) 1723–1732.
[43] M. Mathlouthi, B. Roge, Water vapour sorption isotherms and the caking of food powders, Food Chem. 82 (1) (2003) 61–71.
[44] L.C. Sogutoglu, F. Birkelbach, A. Werner, H. Fischer, H. Huinink, O. Adan, Hydration of salts as a two-step process: water adsorption and hydrate formation, Thermochim. Acta 695 (2021) 178819.
[45] L.C. Sogutoglu, M. Steiger, J. Houben, D. Biemans, H.R. Fischer, P. Donkers, H. Huinink, O.C.G. Adan, Understanding the hydration process of salts: the impact of a nucleation barrier, Cryst. Growth Des. 19 (4) (2019) 2279–2288.
[46] M. Steiger, K. Linnow, H. Juling, G. Gulker, A. El Jarad, S. Bruggerhoff, D. Kirchner, Hydration of $MgSO_4{\cdot}H2O$ and generation of stress in porous materials, Cryst. Growth Des. 8 (1) (2008) 336–343.
[47] J.H. Christian, C.A. Klug, M. DeVore, E. Villa-Aleman, B.J. Foley, N. Groden, A.T. Baldwin, M.S. Wellons, Characterizing the solid hydrolysis product, $UF_4(H_2O)_{2.5}$, generated from neat water reactions with UF_4 at room temperature, Dalton Trans. 50 (7) (2021) 2462–2471.
[48] L.A. Giannuzzi, M. DeVore, M. Summer, M. Wellons, Micromanipulation, FIB, STEM, EDS and EELS of UF_4 particles, Microsc. Microanal. 25 (S2) (2019) 1584–1585.
[49] D. Briggs, M.P. Seah, Practical Surface Analysis. Vol. 1: Auger and X-ray Photoelectron Spectroscopy, 2nd ed., John Wiley & Sons, Chichester, 1990.
[50] X. Feng, B. D'Souza, J. Zhang, Uranium tetrafluoride (UF_4) powder analyzed by XPS, Surf. Sci. Spectra 26 (2) (2019) 024008.
[51] E.S. Ilton, P.S. Bagus, XPS determination of uranium oxidation states, Surf. Interface Anal. 43 (13) (2011) 1549–1560.
[52] E. Thibaut, J.P. Boutique, J.J. Verbist, J.C. Levet, H. Noel, Electronic structure of uranium halides and Oxyhalides in the solid-state. An X-ray photoelectron spectral study of bonding ionicity, J. Am. Chem. Soc. 104 (20) (1982) 5266–5273.
[53] T.L. Barr, S. Seal, Nature of the use of adventitious carbon as a binding-energy standard, J. Vac. Sci. Technol., A 13 (3) (1995) 1239–1246.
[54] A. Froideval, M. Del Nero, R. Barillon, J. Hommet, G. Mignot, pH dependence of uranyl retention in a quartz/solution system: an XPS study, J. Colloid Interface Sci. 266 (2) (2003) 221–235.
[55] M. Schindler, F.C. Hawthorne, M.S. Freund, P.C. Burns, XPS spectra of uranyl minerals and synthetic uranyl compounds. I: the U 4f spectrum, Geochim. Cosmochim. Acta 73 (9) (2009) 2471–2487.
[56] T. Vitova, I. Pidchenko, S. Biswas, G. Beridze, P.W. Dunne, D. Schild, Z.M. Wang, P.M. Kowalski, R.J. Baker, Dehydration of the uranyl peroxide Studtite, $[UO_2(\eta^2\text{-}O_2)(H_2O)_2]{\cdot}2H_2O$, affords a drastic change in the electronic structure: a combined X-ray spectroscopic and theoretical analysis, Inorg. Chem. 57 (4) (2018) 1735–1743.
[57] A.C. Larson, D.T. Cromer, R.B. Roof, Crystal structure of UF_4, Acta Crystallogr. 17 (5) (1964) 555–558.
[58] G.M. Zadneprovskii, S.V. Borisov, Crystal structure of $UF_4{\cdot}2.5H_2O$, Zh, Strukt. Khim. 12 (5) (1972) 831–839.
[59] R. Kips, A.J. Pidduck, M.R. Houlton, A. Leenaers, J.D. Mace, O. Marie, F. Pointurier, E.A. Stefaniak, P.D.P. Taylor, S. Van den Berghe, P. Van Espen, R. Van Grieken, R. Wellum, Determination of fluorine in uranium oxyfluoride particles as an indicator of particle age, Spectrochim. Acta, Part B 64 (3) (2009) 199–207.